

Multivariate fuzzy hidden Markov chains model applied to unsupervised multiscale SAR image segmentation

Cyril Carincotte, Stéphane Derrode and Salah Bourennane

GSM Group - Fresnel Institute (CNRS UMR 6133)

D. U. de St Jérôme - F-13397 Marseille Cedex 20

cyril.carincotte@fresnel.fr

Abstract—This paper deals with unsupervised segmentation of multi-component images. In order to address the classification issue, we propose to use a new vectorial fuzzy version of Hidden Markov Chains (HMC). The main characteristic of the proposed model is to simultaneously use Dirac and Lebesgue measures at the class chain level. It then allows the coexistence of crisp pixels (obtained with the uncertainty measure of the model) and fuzzy pixels (obtained with the fuzzy measure of the model) in the same image. Crisp and fuzzy multi-dimensional densities can then be estimated in the segmentation process, according to the assumption considered to model the statistical links between the layers of the multi-band image. The efficiency of the proposed method is illustrated with a multiscale decomposition of a Synthetic Aperture Radar (SAR) image and comparisons with one-dimensional fuzzy HMC are also provided. The segmentation results show the interest of the new method.

I. INTRODUCTION

The aim of this paper is to present a vectorial fuzzy HMC model for unsupervised segmentation of multi-component images. Such vectorial images can be obtained, e. g. from different channels (multi-spectral or color images), from several sensors (multi-sensor), from images taken at various dates (multi-temporal), or from multiscale analysis of the image of interest. Each component exhibits different characteristics of the spatial scene and the motivation for this work is to combine, in a fuzzy Markov model, the respective information of each image (layer) in order to improve the segmentation.

Indeed, to cope with multivariate situations, HMC based models have been used successfully. However, most of existing methods for automatic multi-band image segmentation, based or not on Markovian assumption, employ deterministic models and consequently neglect the scene fuzziness behavior. These methods, thus, do not take into account the fuzzy multi-component information and may fail to reach a satisfied reliability level in complex situations. In multi-component case, it is interesting not only to take into account the uncertainty measure of the noisy observation (characteristic of probabilistic approach in classical HMC), but also the imprecision measure of this observation (characteristic of fuzzy approaches [1]). By adding a fuzzy measure in a statistical model, we obtain an original model, different from both classical and fuzzy models. Indeed, it preserves the robustness of the statistical segmentation (based on measures of uncertainty), and enriches it with the fuzzy characteristic (measure of imprecision).

This integration has already been done in multi-component HMMRF context [2]. In this work, we propose to extend

the fuzzy HMC model introduced in [3] to the multivariate context, and present its application to unsupervised multiscale image segmentation. The remaining of the paper is organized as follows: first of all, the vectorial fuzzy HMC structure for unsupervised image segmentation is presented in Sec. II. The unknown parameters estimation of the fuzzy Markov chain, achieved with an extension of the Iterative Conditional Estimation (ICE) method [4] to the context considered here, is then presented in Sec. III. Sec. IV is devoted to multi-dimensional densities estimation. Assumptions regarding the bands of the vectorial image are presented, and corresponding crisp and fuzzy parameters estimations are detailed. Finally, Sec. V presents segmentation results obtained with multiscale SAR image and a comparison with the one-dimensional fuzzy HMC model is also provided. Conclusion and perspectives are drawn in Sec. VI.

II. VECTORIAL FUZZY HIDDEN MARKOV CHAINS

In image segmentation, the aim is to reconstitute a thematic map (\mathbf{x}) from a noisy observation (\mathbf{y}). To that goal, Markovian models have been used successfully in a number of situations: radar images segmentation [5], medical images classification [6], change detection context, ... This success is due to the fact that when the unobservable process \mathbf{X} can be modelled by a finite Markov process and when the noise is not too complex, then \mathbf{X} can be recovered from the observed process \mathbf{Y} using different Bayesian classification techniques like Maximum A Posteriori (MAP), or Maximal Posterior Mode (MPM).

In HMC context, the unobservable process \mathbf{X} is modelled by a finite Markov chain $\mathbf{X} = \{X_1, \dots, X_N\}$. In the following, \mathbf{x} will denote a realization of process \mathbf{X} . Furthermore, in unsupervised image segmentation based on HMC, the 2D image needs to be converted in a 1D sequence. This task can be performed thanks to the use of a Hilbert-Peano scan on the image. The Hilbert-Peano scan presents the ability to take into account the neighborhood of the pixel of interest [7]. Fig. 1 shows the scan for a 8×8 multi-component image with M layers.

Recently, it has been shown that the HMC model can, in some particular situations, compete with HMMRF based methods in terms of classification accuracy, while being much faster, even though the latter provides a finer and more intuitive modelling of spatial relationships [5]. Furthermore, HMMRF parameters estimation can often be very complex, which is

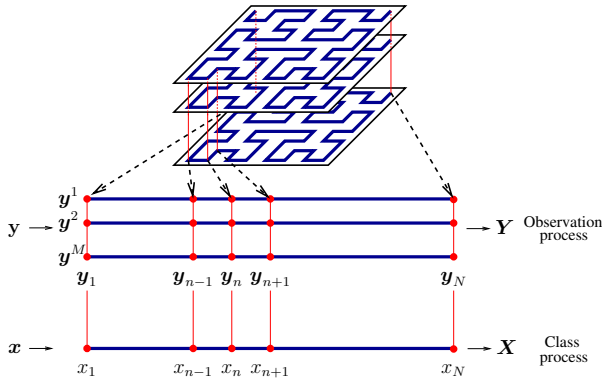


Fig. 1. Hilbert-Peano scan for a 8×8 multi-component image (M = number of layers in the image, N = number of pixels in each layer).

an obvious drawback for practical image analysis, whereas in HMC based methods, the complexity involved in the estimation is mainly dependent on the size and dimensionality of the observations. HMC based methods have thus a real potential for image analysis issues [8].

A. Fuzzy Markov chains model

So, let consider a multi-component image of M layers. According to the Hilbert-Peano scan, we get N series of M data, denoted by $\mathbf{y} = \{\mathbf{y}_1, \dots, \mathbf{y}_N\}$, where $\mathbf{y}_n = \{y_n^1, \dots, y_n^M\}^t$, $1 \leq n \leq N$.

In classical HMC approach, the aim is to classify each $\mathbf{y}_n \in \mathbb{R}^M$ into a set of K classes, the state space $\Omega = \{w_1, \dots, w_K\}$, in order to obtain the segmented chain $\mathbf{x} = \{x_1, \dots, x_N\}$ (see Fig. 1). The segmented image is then reconstructed from \mathbf{x} using an inverse Hilbert-Peano scan.

For the sake of simplicity, we confine our study to the $K = 2$ case, i.e. $\Omega = \{0, 1\}$ (see Remark 1).

In fuzzy HMC context, the range of x_n is now the interval $\Omega = [0, 1]$. In the following, ε_n will denote a realization of random variable X_n and we will adopt the notation:

- $\varepsilon_n = 0$ if the pixel is from class 0,
- $\varepsilon_n \in]0, 1[$ if the pixel is a fuzzy one,
- $\varepsilon_n = 1$ if the pixel is from class 1.

B. Probabilities in fuzzy Markov chains context

As stated previously, each x_n takes its value in two types of sets:

- a hard one $\{0, 1\}$, and
- a fuzzy one defined over the range $]0, 1[$.

Let δ_0 and δ_1 be Dirac weights on 0 and 1, and ν_1 the Lebesgue measure on $]0, 1[$. By taking $\nu = \delta_0 + \delta_1 + \nu_1$ as a measure on Ω , the distribution of X_n can be defined by a density h on Ω with respect to ν .

Remark 1: In fact, the general K classes case implies the definition of a measure ν on $[0, 1]^K$, which is far from being trivial. To our knowledge, one of the simplest approach to address the $K = 3$ classes case has been briefly presented in [9], and then used only in HMRF [6] and HMC context [10].

If we assume that \mathbf{X} is homogeneous and the distribution of each X_n is uniform on the fuzzy class, $P(X_n = \varepsilon_n) = h(\varepsilon_n) = \pi_{\varepsilon_n}$ can be written:

$$\begin{aligned} h(\varepsilon_n = 0) &= \pi_0, \\ h(\varepsilon_n = 1) &= \pi_1, \\ h(\varepsilon_n) &= \pi]_{0,1}[, \forall \varepsilon_n \in]0, 1[, \end{aligned}$$

with $\pi_0 + \pi_1 + \pi]_{0,1}[= 1$.

We can now detail the new expression for the transition probabilities of the Markov chain $t_{\varepsilon_{n-1}, \varepsilon_n}$:

$$\begin{aligned} t_{\varepsilon_{n-1}, \varepsilon_n} &= P(X_n = \varepsilon_n | X_{n-1} = \varepsilon_{n-1}) = \\ &P(X_n = 0 | X_{n-1} = \varepsilon_{n-1}) \delta_0(\varepsilon_n) \\ &+ P(X_n = \varepsilon_n | X_{n-1} = \varepsilon_{n-1}) 1]_{0,1}(\varepsilon_n) \\ &+ P(X_n = 1 | X_{n-1} = \varepsilon_{n-1}) \delta_1(\varepsilon_n). \end{aligned}$$

$\forall \varepsilon_{n-1}, \varepsilon_n \in \Omega$ and $\forall n \in \{2, \dots, N\}$, with

$$t_{\varepsilon_{n-1}, \varepsilon_n} \geq 0 \quad \text{and} \quad \int_{\Omega} t_{\varepsilon_{n-1}, \varepsilon_n} d\varepsilon_{n-1} = 1$$

Similarly to classical HMC, we get:

$$P(\mathbf{X} = \mathbf{x}) = \pi_{\varepsilon_1} \prod_{n=2}^N t_{\varepsilon_{n-1}, \varepsilon_n}.$$

C. Multi-component fuzzy HMC implementation

The approach developed here consists in assuming that ε_n is a realization of a random variable X_n , and each \mathbf{y}_n is a realization of a random vector $\mathbf{Y}_n = \{Y_n^1, \dots, Y_n^M\}^t$. Thus the problem is to estimate the unobserved realization \mathbf{x} of a random process \mathbf{X} from the observed realization \mathbf{y} of a random process $\mathbf{Y} = \{\mathbf{Y}_1, \dots, \mathbf{Y}_N\}$.

Similarly to classical HMC, multi-component fuzzy HMC based image segmentation methods consider the two following assumptions:

- H_1 : the random variables $\mathbf{Y}_1, \dots, \mathbf{Y}_N$ are independent conditionally on \mathbf{X} ;
- H_2 : the distribution of each \mathbf{Y}_n conditionally on \mathbf{X} is equal to its distribution conditionally on X_n .

It is important to note that the random variables $(Y_n^m)_{1 \leq m \leq M}$ are not assumed to be mutually independent conditionally on X_n .

Assuming that distributions of $(X_n, \mathbf{Y}_n, X_{n+1}, \mathbf{Y}_{n+1})$ are independent of n , each state ε_n of the state space (i.e. hard classes $\{0, 1\}$, as well as the fuzzy class $]0, 1[$) is associated to a distribution characterizing the M -dimensional observations \mathbf{y}_n :

$$f_{\varepsilon_n}(\mathbf{y}_n) = P(\mathbf{Y}_n = \mathbf{y}_n | X_n = \varepsilon_n). \quad (1)$$

Given an observed sequence $\mathbf{y} = \{\mathbf{y}_1, \dots, \mathbf{y}_N\}$, the joint state-observation probability is given by:

$$P(\mathbf{X} = \mathbf{x}, \mathbf{Y} = \mathbf{y}) = \pi_{\varepsilon_1} f_{\varepsilon_1}(\mathbf{y}_1) \prod_{n=2}^N t_{\varepsilon_{n-1}, \varepsilon_n} f_{\varepsilon_n}(\mathbf{y}_n).$$

In unsupervised classification, the distribution $P(\mathbf{X} = \mathbf{x}, \mathbf{Y} = \mathbf{y})$ is unknown and must first be estimated

in order to apply a Bayesian classification technique (MAP or MPM). Therefore the following sets of parameters need to be estimated:

- 1) The set Γ characterizing the fuzzy Markov chain parameters, i.e. the initial probability vector $\boldsymbol{\pi} = \{\pi_\varepsilon\}_{\forall \varepsilon \in \Omega}$ and the transition probabilities $\{t_{\varepsilon_{n-1}, \varepsilon_n}\}_{\forall \varepsilon_{n-1}, \varepsilon_n \in \Omega}$.
- 2) The set Δ regrouping the parameters of the M -dimensional distributions presented in (1), i.e. the distributions associated with the hard classes and the fuzzy one.

III. FUZZY MARKOV CHAIN PARAMETERS ESTIMATION

For the estimation of the parameters in Γ , we propose to use an adaptation of the general ICE algorithm [4] which is an alternative to the well-known Estimation-Maximization (EM) algorithm. In fact, ICE does not refer to the likelihood, but it is based on the conditional expectation of some estimators from the complete data (\mathbf{x}, \mathbf{y}) . It is an iterative method which produces a sequence of estimations θ^q of parameter θ as follows:

- 1) initialization θ^0 , obtained with an initial segmentation algorithm (k -means algorithm).
- 2) computation of $\theta^{q+1} = E_q[\hat{\theta}(\mathbf{X}, \mathbf{Y}) \mid \mathbf{Y} = \mathbf{y}]$, where $\hat{\theta}(\mathbf{X}, \mathbf{Y})$ is an estimator of θ .
- 3) Stop the algorithm when $\theta^{Q-1} \approx \theta^Q$.

This section is not intended to give a complete description of the ICE algorithm in the HMC context, interested readers may consult [5].

Similarly to the classical case, parameters in Γ can be calculated analytically by using the Baum-Welch algorithm [11]:

- for the hard classes, the classical normalized Baum-Welch probabilities [12] can be used directly.
- for the fuzzy class, the forward and backward probabilities are defined by:

$$\begin{aligned} \alpha_{n+1}(\xi) &\propto f_\xi(\mathbf{y}_{n+1}) \int_{[0,1]} \alpha_n(\zeta) t_{\zeta, \xi} d\zeta, \\ \beta_n(\xi) &\propto \int_{[0,1]} \beta_{n+1}(\zeta) t_{\xi, \zeta} f_\zeta(\mathbf{y}_{n+1}) d\zeta. \end{aligned} \quad (2)$$

The integrals above can not be calculated analytically and numerical integration must be performed. Hence, the continuous interval $]0,1[$ is partitioned into a given number F of sub-intervals. We thus reduce the domain of fuzzy membership degree $]0,1[$ to F attributed values, corresponding to the medium value of the sub-interval of interest (see Fig. 2), thus resulting in a quantization of the fuzzy measure $]0,1[$. The bigger F is, the closer it is from (2), at the expense of an increase in the computation time.

IV. MULTI-DIMENSIONAL DENSITY ESTIMATION

At each ICE iteration, we need to estimate the multi-dimensional densities $f_{\varepsilon_n}(\mathbf{y}_n)$. Several strategies from multivariate data analysis are available, depending on the assumptions made on the statistical links between the layers, and on the choice of the shape of the one-dimensional densities.

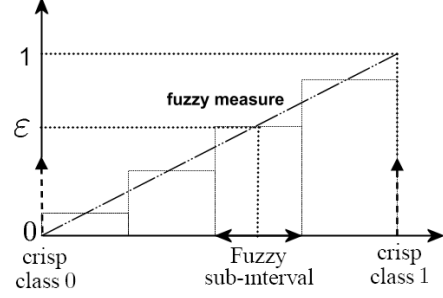


Fig. 2. Partition of the continuous interval $]0,1[$ into $F = 4$ sub-intervals. The attributed values ε correspond to the medium value of the sub-interval of interest.

A. Independence assumption

If independence between the layers is assumed, $f_{\varepsilon_n}(\mathbf{y}_n)$ is the product of M densities $g_{\varepsilon_n}^1, \dots, g_{\varepsilon_n}^M$ defined on \mathbb{R} :

$$f_{\varepsilon_n}(\mathbf{y}_n) = \prod_{m=1}^M g_{\varepsilon_n}^m(y_n^m).$$

For example, if we consider that $f_{\varepsilon_n}(\mathbf{y}_n)$ are multi-dimensional Gaussian densities, parameters estimation can be easily achieved from the first and second moments of a M -dimensional sample. Denoting by $\mathcal{N}(m, \sigma^2)$ the normal distribution with mean m and variance σ^2 , the pdf of the hard classes are then expressed according to:

$$\begin{aligned} \varepsilon_n = 0 &: \mathcal{N}(m_0, \sigma_0^2), \\ \varepsilon_n = 1 &: \mathcal{N}(m_1, \sigma_1^2). \end{aligned}$$

The parameters $\Delta = \{m_0, m_1, \sigma_0, \sigma_1\}$ can be estimated by computing the empirical mean of several estimates according to $\theta^{q+1} = \frac{1}{L} \sum_{l=1}^L \hat{\theta}(\mathbf{x}^l, \mathbf{y})$, where \mathbf{x}^l is an *a posteriori* realization of \mathbf{X} conditionally on \mathbf{Y} . It can be shown that $\mathbf{X} \mid \mathbf{Y}$ is a non homogeneous Markov chain whose parameters can be computed from the forward and backward probabilities presented in Sec. III.

The definition of the fuzzy measure \bar{A} : “the pixel belongs to class 1” corresponding to the fuzzy class $]0,1[$, and its fuzzy membership function μ_A , allows us to estimate the fuzzy parameters of the set Δ in this new context. The proposed fuzzy membership function μ_A is defined by:

$$\mu_A(m) = \begin{cases} 1 - \frac{m_1 - m}{m_1 - m_0} & \forall m \in [m_0, m_1], \\ 0 & \text{elsewhere.} \end{cases}$$

Accordingly, the parameters of the Gaussian pdf for the fuzzy class can then be estimated by:

$$\begin{aligned} m_{\varepsilon_n} &= (1 - \varepsilon_n) m_0 + \varepsilon_n m_1, \\ \sigma_{\varepsilon_n} &= (1 - \varepsilon_n)^2 \sigma_0^2 + \varepsilon_n^2 \sigma_1^2. \end{aligned} \quad (3)$$

Remark 2: In a number of image modalities, such as in SAR, sonar or Magnetic Resonance Image (MRI), the noise can not be properly modeled by Gaussians laws. Moreover, the nature and the form of the distribution of each class can vary in the different layers.

Indeed, in this study, experiments have been conducted with Gamma distributions. These distributions can be expressed with the four moments of order 1, 2, 3 and 4. In this case, moments of higher order can then be estimated by the extension of (3) to the considered order. The estimation of those higher order moments is also tractable in Sec. IV-B.

B. PCA approach

However, most of the time, layers of a vectorial image can not be considered mutually independent, and the statistical links between the layers should be used to improve the segmentation.

When dependence is assumed to moments of order less than 2, a solution consists in applying a Principal Component Analysis (PCA) algorithm on the data before densities estimation [13]. This can be done by projecting \mathbf{y}_n onto an orthonormal system defined by \mathbf{W} for each class, so that the new data $\mathbf{t}_n = \mathbf{W}\mathbf{y}_n$ are decorrelated. Hence, we get the following estimation:

$$f_{\varepsilon_n}(\mathbf{y}_n) = |\det(\mathbf{W}_{\varepsilon_n})| \prod_{m=1}^M g_{\varepsilon_n}^m(t_n^m). \quad (4)$$

For the hard classes, the parameters $\Delta = \{m_0, m_1, \Gamma_0, \Gamma_1\}$ are also estimated thanks to an *a posteriori* realization of $\mathbf{X} | \mathbf{Y}$. $(\mathbf{W}_0, \mathbf{W}_1)$ are estimated thanks to the Cholesky decomposition C , by: $\mathbf{W}_0^t = (C(\Gamma_0))^{-1}$, with Γ_0 the covariance matrix of the observed data corresponding to the class 0 in $\mathbf{x} | \mathbf{y}$, and symmetrically for \mathbf{W}_1 .

For the fuzzy class, the estimation of $\mathbf{W}_{\varepsilon_n}$ can not be achieved analytically due to the fact that the observation data corresponding to the fuzzy class are not known. One possible way to carry out the estimation is to directly extend (3) to Γ_{ε_n} [2], with $\forall \varepsilon_n \in]0, 1[$:

$$\begin{aligned} m_{\varepsilon_n} &= (1 - \varepsilon_n) m_0 + \varepsilon_n m_1, \\ \Gamma_{\varepsilon_n} &= (1 - \varepsilon_n)^2 \Gamma_0^2 + \varepsilon_n^2 \Gamma_1^2. \end{aligned}$$

These estimations of the M -dimensional densities allow to implement this new vectorial fuzzy HMC model in an unsupervised way. Next section presents the application of this model to unsupervised fuzzy image segmentation of multiscale SAR images.

V. MULTISCALE SAR IMAGE SEGMENTATION

Fig. 3 shows an excerpt of an ASAR ENVISAT image acquired on November 17th, 2002, four days after *Prestige* wreck near the Portuguese coast. In order to perform the multivariate fuzzy HMC classification of this SAR observation, Fig. 3 is first transformed into a multi-component image thanks to a multiscale decomposition.

A. Multiscale decomposition

For the sake of brevity and due to the fact this model is not restricted to multiscale images segmentation, we only present the multiscale analysis used in the experiments.

The multiscale analysis allows us to outline local texture characteristics at different wavelengths. Such multiscale decomposition has been used successfully in oil slick segmentation in SAR context [14]. In this application, the wavelet used has been defined in [15], for which only two wavelet filters are required:

$$\begin{aligned} \theta(x, y) &= \theta(x)\theta(y), \\ \psi^{hori}(x, y) &= \frac{\partial\theta(x, y)}{\partial x} \quad \text{and} \quad \psi^{vert}(x, y) = \frac{\partial\theta(x, y)}{\partial y}, \end{aligned}$$

where the primitive $\theta(\cdot)$ is a cubic spline with Fourier transform given by:

$$\hat{\theta}(w) = \left(\frac{\sin(w/4)}{w/4} \right)^3.$$

By denoting L the number of decompositions, the multiscale image is obtained by L iterative convolutions with filters defined by $\theta(\cdot)$, $\psi^{hori}(\cdot)$ and $\psi^{vert}(\cdot)$. The obtained multiscale image is thus composed of:

- one layer corresponding to the low-pass (approximated) image, and
- $2 \times L$ layers of wavelet coefficients (horizontal and vertical).

The obtained images contain the same information as the original one, only the way to characterize the information has changed. Fig. 4 shows the three sub-bands obtained from the multiscale decomposition of Fig. 3 with $L = 1$.

B. Experimental protocol

In this application, the “oil slick” and the “free sea” were naturally considered as crisp class 0 and crisp class 1. The fuzzy measure \bar{A} thus corresponds to: “the pixel belongs to the free sea class”. The segmentation results depend on the partition of $]0, 1[$; the choice of the F sub-intervals implies different values of fuzzy measure ε , e.g. $F = 2$ implies $\varepsilon \in$

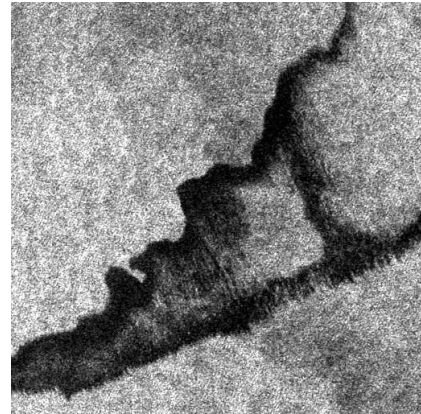


Fig. 3. ASAR ENVISAT excerpt (512×512) acquired on November 17th, 2002, after *Prestige* wreck (Wide Swath mode, orbit: 3741), ©ESA.

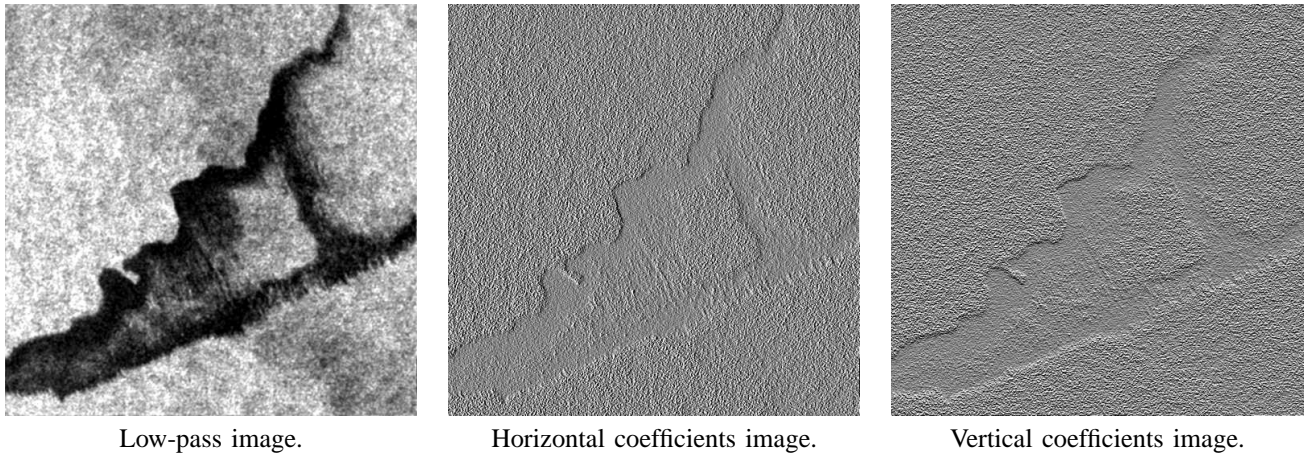


Fig. 4. Multiscale decomposition images of Fig. 3 with $L = 1$ (see text in Sec. V-A).

$\{0.25, 0.75\}$, $F = 4$ implies $\varepsilon \in \{0.125, 0.375, 0.625, 0.875\}$ (see Fig. 2). Pixel intensities are thus proportional to ε ; bright intensities representing high proportion of “free sea”, and dark ones representing high proportion of “oil slick”.

In order to make valuable comparisons, multivariate fuzzy HMC classifications of Fig. 4 was compared with corresponding one-dimensional one [3] of Fig. 3.

In all experiments, parameters initialization was done with a k -means classifier. The ICE algorithm was stopped after 50 iterations, assuming it has converged, and the image classification was performed with respect to the fuzzy MPM criterion [9]. $f_{\varepsilon_n}(y_n)$ were supposed to be one-dimensional Gamma densities in one-dimensional fuzzy HMC case, and the product of M Gamma ones in the multivariate case (in our case $M = 3$). Finally, for the vectorial fuzzy HMC, the correlation assumption was made, and ACP approach was adopted.

C. Segmentation results

Fig. 3 and 4 contain two major difficulties: first, oil on the water reduces air-sea interaction; the main observable phenomenon is the dampening of the capillary (surface) waves, which causes the major part of the image noise [16]. Secondly,

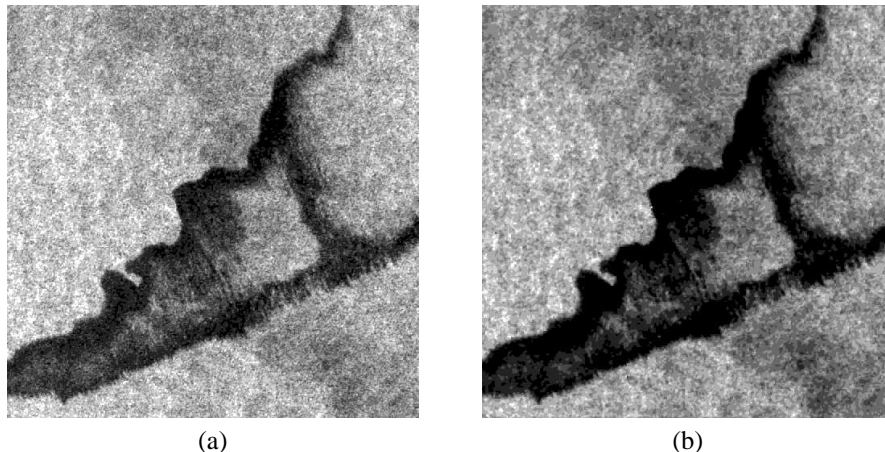


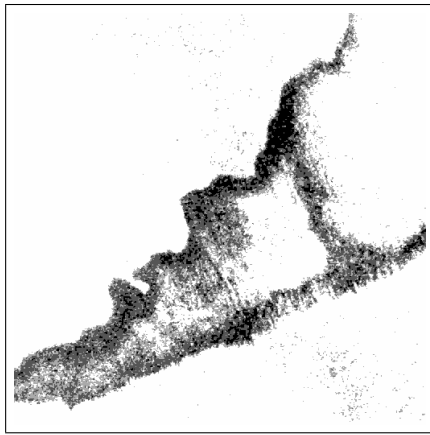
Fig. 5. Segmentation results obtained with one-dimensional (a) and multivariate (b) fuzzy HMC for $F = 6$ sub-intervals.

TABLE I
COMPUTATION TIMES (SEC.) CORRESPONDING TO FUZZY HMC AND
MULTIVARIATE FUZZY HMC RESULTS PRESENTED IN FIG. 5.

Model	Init.	ICE algo.	MPM classif.
Fuzzy HMC	73	1871	28
Multivariate fuzzy HMC	123	4207	69

one distinguishable area seems to appear in the image, from right bottom corner to middle up. This zone is due to weak surface wind, which leads to low radar backscattering.

Fig. 5 shows segmentation results obtained with both models for $F = 6$ sub-intervals, and Tab. I presents corresponding computation times. As it could be expected, the computational complexity involved in the multivariate model is quite higher than the one involved in the classical one. One can observe that a big number of fuzzy sub-intervals provides a fine characterization of the observed scene. Furthermore, the segmentation results produced by the fuzzy vectorial HMC model is more homogeneous. The global shape and frontiers of the oil slick seem to be better defined. It is obvious that those differences



(a) Deffuzzification result of Fig. 5-(a)



(b) Deffuzzification result of Fig. 5-(b)

Fig. 6. Deffuzzification results of images in Fig. 5 ($\eta = 0.4$).

are due to the way the multivariate information is characterized in the multiscale image.

Concerning the oil slick detection, a basic defuzzification technique has been processed on Fig. 5 in order to reveal its shape. Since the values of fuzzy measure ε correspond to the membership degree of the hard class 1 (free sea), a defuzzification was defined according to: if $\varepsilon > \eta$, $\varepsilon = 1$. Fig. 6 presents the defuzzification results of Fig. 5 for $\eta = 0.4$.

We can observe in Fig. 6-(b) that only few pixels related to the weak surface wind phenomenon have been taken into account in the segmentation process of multivariate fuzzy HMC. Nevertheless, this model clearly characterizes the frontiers of the oil slick. In fact, the rude defuzzification applied seems to produce a reliable segmentation of the oil slick, and then illustrates the interest of the vectorial fuzzy HMC model.

VI. CONCLUSION

In this work, a new fuzzy vectorial HMC model has been presented, with application to unsupervised multiscale SAR image segmentation. The main contribution of this work was the integration of a fuzzy measure in a vectorial HMC model. It then allows the coexistence of crisp pixels (obtained with the uncertainty measure of the model) and fuzzy pixels (obtained with the fuzzy measure of the model) in the same multiband image. Correlation assumption was considered to model the statistical links between the pixels in the layers, and to estimate crisp and fuzzy multi-dimensional densities.

Experimental results confirm the validity of the proposed approach. The vectorial fuzzy HMC model seems to be promising in the field of multi-component image segmentation, due to the imprecision measure ability to take into account the multivariate information. From this work, we plan to study the high-order dependence case between the layers (by replacing PCA matrix by ICA one).

ACKNOWLEDGMENT

The authors are grateful to G. Mercier from the GET/ENST Bretagne for valuable discussions on oil slick characteristics

and multiscale analysis approach.

REFERENCES

- [1] L. A. Zadeh, "Fuzzy logic," *IEEE Trans. Comput.*, vol. 21, no. 4, pp. 83–93, April 1988.
- [2] F. Salzenstein, C. Collet, and M. Petremand, "Fuzzy Markov random fields for multispectral images - Champs de Markov flous pour images multispectrales," *Trait. Signal*, vol. 21, no. 1, pp. 37–54, 2004, in french.
- [3] C. Carincotte, S. Derrode, G. Sicot, and J. M. Boucher, "Unsupervised image segmentation based on a new fuzzy hidden Markov chain model," in *IEEE Int. Conf. Acoust., Speech, Signal Processing*, Montreal, Canada, May 17-21 2004.
- [4] W. Pieczynski, "Statistical image segmentation," *Mach. Graph. and Vis.*, vol. 1, pp. 261–268, 1992.
- [5] R. Fjørtoft, Y. Delignon, W. Pieczynski, M. Sigelle, and F. Tupin, "Unsupervised segmentation of radar images using hidden Markov chains and hidden Markov random fields," *IEEE Trans. Geosci. Remote Sensing*, vol. 41, no. 3, pp. 675–686, 2003.
- [6] S. Ruan, B. Moretti, J. Fadili, and D. Bloyet, "Fuzzy Markovian segmentation in application of magnetic resonance images," *Comp. Vis. and Im. Under.*, vol. 85, pp. 54–69, 2002.
- [7] W. Skarbek, "Generalized Hilbert scan in image printing," in *Theoretical Foundations of Computer Vision*, R. Klette and W. G. Kropetsh, Eds. Berlin: Akademik Verlag, 1992.
- [8] K. Aas, L. Eikvil, and R. Huseby, "Applications of hidden Markov chains in image analysis," *Pat. Recog.*, vol. 32, no. 4, pp. 703–713, 1999.
- [9] F. Salzenstein and W. Pieczynski, "Parameter estimation in hidden fuzzy Markov random fields and image segmentation," *Graph. Mod. and Im. Proc.*, vol. 59, no. 4, pp. 205–220, July 1997.
- [10] C. Carincotte, S. Derrode, and S. Bourennane, "Unsupervised change detection on SAR images using fuzzy hidden Markov chains," *IEEE Trans. Geosci. Remote Sensing*, unpublished.
- [11] L. Rabiner, "A tutorial on hidden Markov models and selected applications in speech recognition," in *Proc. IEEE*, vol. 77, no. 2, Feb. 1989, pp. 257–286.
- [12] P. A. Devijver, "Baum's forward-backward algorithm revisited," *Pattern Recognition Letters*, vol. 39, no. 3, pp. 369–373, december 1985.
- [13] W. Pieczynski, J. Bouvrais, and C. Michel, "Estimation of generalized mixture in the case of correlated sensors," *IEEE Trans. Image Processing*, vol. 9, no. 2, pp. 308–312, 2000.
- [14] G. Mercier, S. Derrode, and W. Pieczynski, "Multiscale oil slicks segmentation - Segmentation multiéchelle de nappes d'hydrocarbure," *Trait. Signal*, vol. 21, no. 4, pp. 329–346, 2004, in french.
- [15] S. Mallat and S. Zhong, "Characterization of signals from multiscale edges," *IEEE Trans. Pattern Anal. Machine Intell.*, vol. 7, no. 14, pp. 710–732, July 1992.
- [16] F. Girard-Arduin, G. Mercier, and R. Garello, "Oil slick detection by SAR imagery: potential and limitation," in *Oceans 2003*, San Diego, USA, september 2003, pp. 22–26.